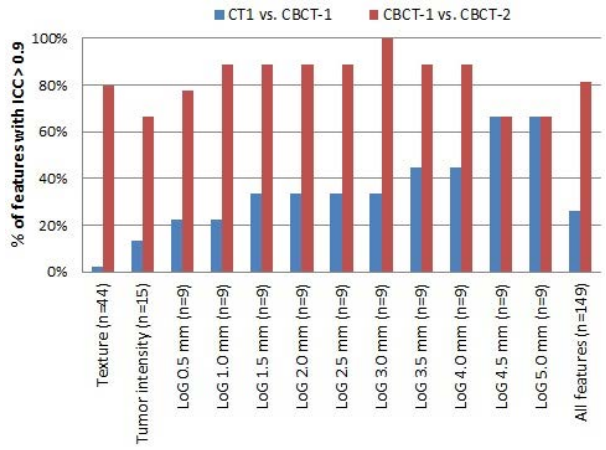

Figure: Percentage of features with ICC>0.9 for CT1 vs. CBCT-1 and CBCT-1 vs. CBCT-2, displayed for each feature group.

Conclusion: For 26% of the radiomics features there is good agreement between CT1 and CBCT. 81% of the image features show high correlation between CBCT-FX1 and CBCT-FX2 where no large differences are expected. In the future, radiomic features derived from CBCT images will be investigated to monitor changes of CBCT features over the course of treatment. One has to be careful with mixing radiomic features derived on planning CT and CBCT scans.

PO-0923

Comparing FMISO and FDG positive tumour sub-volumes for PET-based dose escalation in SCCHN

D. Mönnich[1], S. Leibfarth[1], S. Welz[2], C. Pfannenberg[3], D. Zips[2], D. Thorwarth[1]
[1]*Section for Biomedical Physics - Department of Radiation Oncology, University Hospital Tübingen, Tübingen, Germany*
[2]*Department of Radiation Oncology, University Hospital Tübingen, Tübingen, Germany*
[3]*Department of Diagnostic and Interventional Radiology, University Hospital Tübingen, Tübingen, Germany*

Purpose or Objective: Tumour sub-volumes for dose escalation can be defined using different PET tracers. This study compares hypoxic volumes defined by FMISO PET and metabolically active volumes defined by FDG PET for patients with advanced squamous cell carcinomas of the head and neck (SCCHN).

Material and Methods: Imaging data of 14 patients was used, which were included in a phase II FMISO dose escalation study. Pre-therapy FMISO PET/CT images were acquired four hours post tracer injection. FDG PET/CT imaging was performed according to the institutional diagnostic protocol. The planning CT and the GTV of the primary tumour were available. Datasets were deformably co-registered using the CT images. Metabolically active sub-volumes were segmented in FDG PET images based on a source-to-background method with an adaptive threshold. Hypoxic sub-volumes were defined using a tumour-to-muscle threshold of 1.4. Expanding the volumes by an isotropic margin of five millimeters resulted in PTV-prim and potential dose escalation volumes PTV-FMISO and PTV-FDG. We analyzed the overlap between PTV-FMISO and PTV-FDG.

Results: Mean dose escalation volumes were 19.7 cm^3 (0.0-57.3 cm^3) for PTV-FMISO and 39.3 cm^3 (17.5-91.9 cm^3) for PTV-FDG. On average PTV-FDG covered 73.5% of PTV-FMISO (4.9-100.0%). Only for two out of fourteen patients (14%) PTV-FMISO was completely covered by PTV-FDG. Vice versa 36.3% of PTV-FDG overlapped with PTV-FMISO (0.0-97.4%). PTV-prim from treatment planning was 111.1 cm^3 (57.1-201.2 cm^3). Detailed results of the overlap analysis for all patients are given in Table 1.

Patient	Volumes			Overlap PTV_{FDG} and PTV_{FMISO}		
n=14	PTV_{prim} / cm^3	PTV_{FDG} / cm^3	PTV_{FMISO} / cm^3	cm^3	% of PTV_{FDG}	% of PTV_{FMISO}
006	65.8	35.6	10.3	9.5	26.8	92.7
007	118.7	42.4	27.1	7.6	17.8	28.0
008	81.6	43.6	54.0	39.4	90.4	73.0
009	142.8	47.6	0.0	0.0	0.0	
010	106.6	34.5	12.1	9.0	26.0	74.0
011	57.3	36.5	0.0	0.0	0.0	
013	74.9	26.6	22.5	21.4	80.3	95.0
014	69.2	21.2	5.9	5.9	27.8	100.0
015	196.3	91.9	33.5	25.5	27.8	76.2
016	201.2	17.9	16.0	0.8	4.4	4.9
017	166.4	43.4	4.8	4.8	11.0	100.0
018	57.1	17.5	13.8	11.4	65.0	82.5
019	117.0	39.1	57.3	38.0	97.4	66.4
020	100.4	51.7	19.3	17.2	33.2	89.0
Mean	111.1	39.3	19.7	13.6	36.3	73.5
Min	57.1	17.5	0.0	0.0	0.0	4.9
Max	201.2	91.9	57.3	39.4	97.4	100.0

Conclusion: PTV-FDG typically covers PTV-FMISO only partially and is on average two times larger. Therefore, a dose escalation in the metabolically active sub-volume partially misses the hypoxic sub-volume. The large volume difference suggests that a substantially higher dose escalation is feasible in PTV-FMISO than in PTV-FDG. Clinical trials are required to compare the efficacy of both methods.

PO-0924

Histogram analysis of ADCs from DWMRI predicts tumour response and survival for rectal cancer

K. Bakke[1], T. Seierstad[2], K.H. Hole[2], S. Dueland[3], K. Flatmark[4], A. Hansen Ree[1], K. Røe Redalen[1]
[1]*Akershus University Hospital, Department of Oncology, Lørenskog, Norway*
[2]*Oslo University Hospital, Department of Radiology and Nuclear Medicine, Oslo, Norway*
[3]*Oslo University Hospital, Department of Oncology, Oslo, Norway*
[4]*Oslo University Hospital, Department of Gastroenterological Surgery, Oslo, Norway*

Purpose or Objective: Patients with locally advanced rectal cancer (LARC) are commonly treated with neoadjuvant chemoradiotherapy (CRT) followed by radical surgery. However, tumor responses vary considerably and about one third of the patients experience poor disease outcome due to metastatic progression. We aimed to investigate if apparent diffusion coefficients (ADCs) quantified from diffusion-weighted MRI (DWMRI) predicted histologic tumor response to the neoadjuvant treatment and long-term survival. Recognizing the tumor heterogeneity we specifically aimed to explore if histogram analysis of tumor ADC may reveal more useful information than the commonly used mean ADC measure.

Material and Methods: Data from 23 prospectively enrolled patients receiving induction neoadjuvant chemotherapy (NACT) followed by CRT and radical surgery was analyzed. DWMRI was acquired at baseline and after NACT. Tumor volumes contoured in T2-weighted MR images were transferred to tumor ADC maps calculated with b-values 300 and 900 s/mm2, before ADCs were extracted from all tumor voxels and presented as histograms. The predictive information contained in the histograms was evaluated using receiver operating characteristic (ROC) curve analysis of each percentile from 1-100. Study endpoints were histologic tumor regression grade (TRG) and 5-year progression-free survival (PFS).

Results: Using the change in tumor ADC from baseline to NACT completion, we identified a histogram area below median (20th–40th percentiles) to be associated with both TRG and PFS. By using the 20th percentile, an increase in

ADC predicted poor histologic tumor response (TRG3–5 versus TRG1–2) with 91% sensitivity and 83% specificity (area under curve (AUC)=0.89, 95% confidence interval (CI)=0.74–1.0, p=0.001). Using the 30th percentile, an increase in ADC predicted poor PFS with 89% sensitivity and 71% specificity (AUC=0.75, 95% CI=0.54–0.95, p=0.051). Univariate regression analysis also revealed that the ADC increase was significantly associated to poor PFS (hazard ratio=9.7, 95% CI=1.21-78.30, p=0.033).

Conclusion: By ADC histogram analysis of DWMRI acquired during NACT of LARC we identified low histogram percentiles as predictive of histologic tumor response in particular, but also long-term survival. The results require validation in larger, independent cohorts, but are promising for identification of patients that may benefit from individualized treatment approaches for improved disease outcome.

PO-0925

Simulation of FMISO diffusion-retention in a three-dimensional tumor model

L.J. Wack[1], A. Menegakis[2], R. Winter[1], S. Böke[2], D. Mönnich[1], D. Zips[2], D. Thorwarth[1]

[1]*University Hospital Tübingen, Department of Radiation Oncology- Section for Biomedical Physics, Tübingen, Germany*

[2]*University Hospital Tübingen, Department of Radiation Oncology, Tübingen, Germany*

Purpose or Objective: Tumor hypoxia is prognostic for poor outcome after radiotherapy (RT). A method for non-invasive assessment of hypoxia is PET using hypoxia radiotracers such as FMISO. The goal of this study was to develop and evaluate a tool to simulate 3D oxygen distribution and the resulting FMISO accumulation on realistic vessel architectures, which can be compared to measured PET activities in small animal experiments.

Material and Methods: Two FaDu tumors (human HNSCC) were grown on the right hind leg of nude mice. Imaging was performed after a growth phase of about 5 weeks. FMISO was injected into the tail vein of the anesthetized mice with an activity of ~12MBq for dynamic PET/MRI. ROIs inside the left ventricle and in the tumor were chosen to determine blood and tumor time activity curves (TACs). After image acquisition tumors were excised, snap frozen and cut into consecutive sections (20µm). Sections were stained with immunoflourescence-labeled antibodies for endothelial marker CD31 and scanned with a Zeiss Axioplan 2 fluorescence microscope. Obtained immunofluorescence images were rigidly registered, manually adjusted and thresholded to create a binary 3D vessel map. These maps were used to simulate 3D oxygen distributions based on a Michaelis-Menten relation. Using the oxygen distribution and the dynamic activity in the left ventricle as input, FMISO retention was simulated on the same vessel maps. A tumor ROI was selected and its average activity at different time points post-injection (p.i.) compared against the measured activity in the same region on the PET scan (tumor TAC). To compare 3D and 2D simulations, the simulation were repeated in 2D on the individual sections, and 2D-based oxygen histograms and TACs were determined.

Results: O2 histograms showed a large difference between 2D and 3D simulations, with much lower values for 2D simulations than for 3D (5.94 mmHg vs 26.57 mmHg). Mean values were closer together (8.9 mmHg vs 13.2 mmHg). This is due to the large amount of anoxic voxels (pO2 < 1 mmHg) in the 2D simulation, which made up 17.5% of all simulated voxels in 2d, but less than 1% in the 3D simulations (see Table 1). Visually, the 3D simulations result in a TAC with a similar overall shape compared to the TAC measured with small animal PET, but with a 20.7% overestimation of activity. However, the 2D simulations severely overestimated the total activity by 99.2% (2D) when compared against measured activity in the tumor after 90min as determined by PET.

	2D simulation	3D simulation	Small animal PET image
Tumor 1			
Median oxygen content (mmHg)	2.11	26.03	n.a.
Mean oxygen content (mmHg)	12.28	15.65	n.a.
Anoxic fraction (<1mmHg)	14.1%	0.0%	n.a.
FMISO activity at 90 min p.i. (kBq/ml)	535.2	460.2	425.3
Tumor 2			
Median oxygen content (mmHg)	9.78	27.79	n.a.
Mean oxygen content (mmHg)	14.14	26.57	n.a.
Anoxic fraction (<1mmHg)	20.9%	1.0%	n.a.
FMISO activity at 90min p.i. (kBq/ml)	1339.0	653.7	491.2

Conclusion: 3D simulations based on real 3D vessel architecture is feasible. Our FMISO simulations showed large discrepancies between 2D and 3D simulation approaches, with the 3D values being closer to the PET measurements. Verification of 3D tracer accumulation patterns in additional tumors against pimonidazole stainings is still necessary to validate and calibrate the method, with PET scans in the same test subject to confirm observed activity.

PO-0926

Voxel-based PSMA-PET/histopathology analysis in patients with primary prostate cancer

C. Zamboglou[1], F. Schiller[2], T. Fechter[1], V. Drendel[3], C.A. Jilg[4], P.T. Meyer[2], M. Mix[2], A.L. Grosu[1]

[1]*Universitätsklinik Freiburg, Klinik für Strahlenheilkunde, Freiburg, Germany*

[2]*Universitätsklinik Freiburg, Klinik für Nuklearmedizin, Freiburg, Germany*

[3]*Universitätsklinik Freiburg, Institut für Pathologie, Freiburg, Germany*

[4]*Universitätsklinik Freiburg, Klinik für Urologie, Freiburg, Germany*

Purpose or Objective: Tumorcontrol of primary prostate cancer (PC) is dose dependent. Dominant index lesions (DIL) within the prostatic gland are responsible for local and distant failure. Radionuclide-labelled inhibitors of prostate-specific membrane antigen (PSMA-PET) showed promising preclinical and clinical results in detection of primary prostate cancer. We correlated PET/histopathology using a new coregistration approach, which allows pixel-wise evaluation of the tracers performance in prostatic tissue. Aim of this work is to evaluate the diagnostic accuracy of 68Ga-PSMA-PET/CT and to determine potential SUV-thresholds enabling a focal dose escalation on DIL delineated by PET.

Material and Methods: 10 patients with primary PC and 68Ga-PSMA-PET/CT were enrolled. After prostatectomy, thorough histopathological preparation and anatomical-based coregistration between in-vivo and ex-vivo material was performed. Simulated PET-images were generated out of blurred 3D histopathological tumor distribution (histoPET). The coregistration was further optimized by matching histoPET information with the in-vivo PET signal. The tracer performance was evaluated by coefficient of determination (R^2) between histoPET/PSMA-PET patterns and SUV-values within different tissue types.

Results: 1 patient was excluded due to imprecise pathological preparation. Mean R^2 value was 60 % (± SD 15.2, range: 42.5-81.6). SUVmax of PSMA-PET was located in non resolution adapated / resolution adapted PC-tissue in 80%/90% of patients. Mean SUVmean in non resolution adapted PC and non-PC tissue was 6.1 (range: 2 – 21) and 2.7 (range: 1.3 – 8.2), respectively. The ratio between SUVmean in PC / non-PC was 2.2 (SD ± 0.6).